Absolute total cross section for electron scattering from molecular hydrogen from 1 to 50 eV

Robert K. Jones
Department of Chemistry, Indiana University, Bloomington, Indiana 47405
(Received 20 July 1984)

A time-of-flight electron transmission spectrometer was employed to measure the absolute total electron-scattering cross section (elastic plus inelastic, integrated over all angles) for molecular hydrogen for incident electron energies from 1 to 50 eV. A complete error analysis is included. Comparisons are made with recent measurements and calculations.

I. INTRODUCTION

The investigation of collision processes plays an essential role in developing basic understanding of atomic and molecular physics. Since the validity of a theory must be judged by how well it predicts experimental results, the measurement of scattering cross sections has become an important task for experimentalists. The scattering of low-energy electrons from molecules can yield interesting information about the electronic structure of the target molecule with relatively simple analysis.[1] Electron-molecule scattering has practical applications to laser development,[2] and the modeling of gaseous dielectrics[3] and magnetohydrodynamic (MHD) plasmas.[4]

Since H_2 is the simplest neutral molecule it has been the most extensively studied theoretically.[5] A number of absolute total cross-section measurements have been made,[6–11] but agreement between them is only marginal, indicating a further need for accurate values.

This paper presents the measurement of the absolute total electron-scattering cross section (TCS) for H_2 (elastic plus inelastic, integrated over all angles) for incident electrons from 1 to 50 eV. A complete error analysis is given. Results are compared with other measurements and recent calculations.

II. APPARATUS AND PROCEDURE

A brief description of the time-of-flight (TOF) electron transmission spectrometer and experimental procedure, with emphasis on recent modifications, is given here. A more complete description can be found in an earlier publication.[12]

The apparatus, represented schematically in Fig. 1, consisted of a broad spectrum, pulsed electron source in line with a sample cell, and electron detector. The electron TOF from source to detector was measured with a time-to-amplitude converter (TAC) and the spectra were stored using a multichannel pulse height analyzer (MCPHA).

Since a number of potential errors were affected by the sample-cell configuration, three different sample cells were employed. Each cell consisted of a closed cylinder with circular apertures at the ends to allow the passage of electrons through a cell. A capacitance manometer was connected at several points along the cell. Each connection had its own shutoff value so the pressure at different locations could be measured and pressure gradients could be determined. The dimensions of the cells that were varied included the cell length, cell diameter, diameter of the aperture nearest the detector (exit aperture), diameter of a skimmer aperture placed in front of the detector to

TABLE I. Sample-cell dimensions.

Dimension	Sample cell I	II	III
Cell length	20 cm	38 cm	38 cm
Cell inner diam.	3.2 cm	2.9 cm	3.2 cm
Exit-aperture inner diam.	2.0 mm	3.0 mm	2.0 mm
Skimmer inner diam.	5.0 mm	3.6 mm	3.8 mm
Distance from exit aperture to skimmer	19.7 cm	1.9 cm	2.7 cm
Angle subtended by detector from the end of the cell	4.85×10^{-4} sr	2.88×10^{-2} sr	1.63×10^{-2} sr

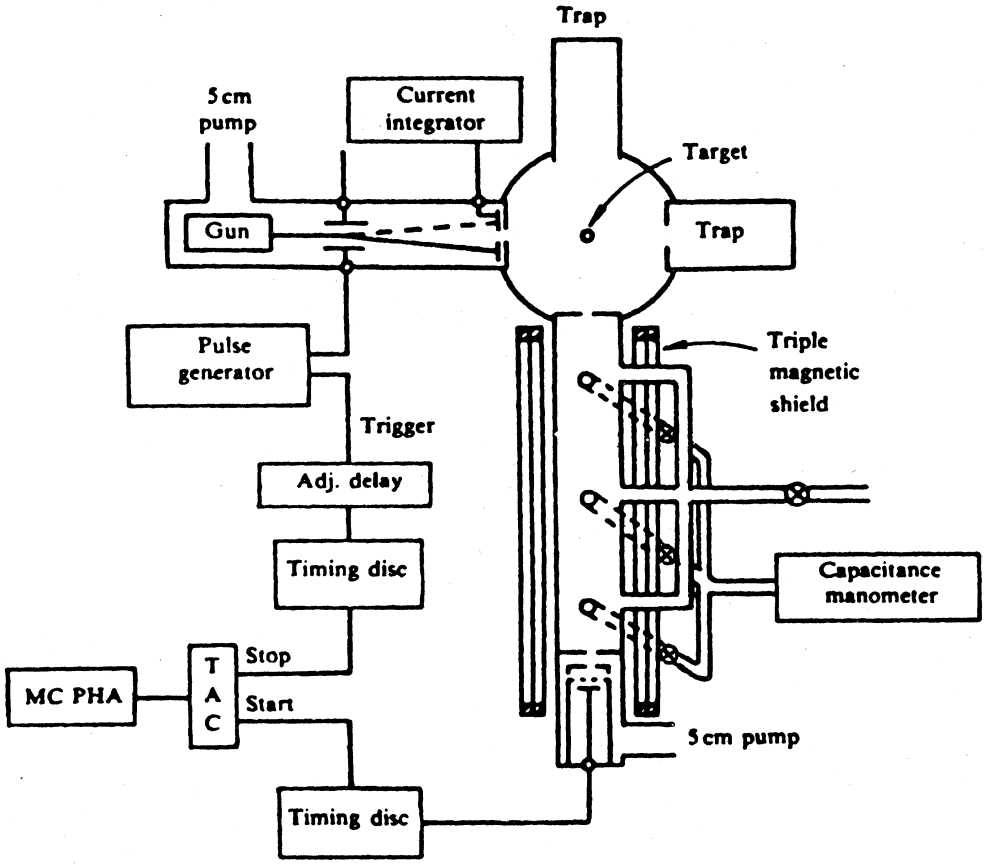

FIG. 1. Time-of-flight apparatus used to measure the total cross section, depicted with sample-cell III. Total flight distance from target to detector is $\approx$45 cm.

reduce the effective solid angle of the detector, and the distance between the exit aperture and skimmer. They are listed in Table I with the solid angle subtended by the detector from a point at the end of the sample cell. In all cases the aperture nearest the electron source (entrance aperture) was 2.0 mm in diameter.

The experimental procedure involved collecting TOF spectra for alternating gas and reference segments. With knowledge of total collection times, sample gas pressure, temperature, and cell length, the absolute total integral cross section was obtained for each energy point using the Beer-Lambert relation

$$Q=(1/nL)\ln(I_0/I)\ , \tag{1}$$

where Q is the total cross section, n is the number density of the sample gas, L is the sample cell length, I_0 is the reference count rate, and I is the gas count rate.

Typical durations for reference and gas segments were 100 and 200 s, respectively. The total time for an experiment was typically six hours. This rapid cycling was facilitated by the complete automation of the experiment. The pressure in the sample cell was continuously recorded and averaged over time and the primary electron beam current was recorded and regulated. The background gas in the region of the electron source and detector was maintained at a constant pressure over both reference and gas segments by diverting the sample gas flow to those regions during the reference segments. This procedure insured that any sample gas effects on the pulsed electron source or detector efficiency were constant over both gas and reference segments.

In order to obtain a count rate from the accumulated counts, a precise knowledge of the collection time was required. Since after the detection of an electron the electronics were temporarily unable to process any further events, an instrument dead time was considered in finding the effective collection time. The dead time was determined for each channel of the MCPHA in the following manner: Since the electron gun was pulsed every 2.5 μs, it was convenient to set the dead time of the electronics equal to a multiple of this period τ. After the detection of an electron the TAC remained dead for the remainder of the current period plus an additional five periods. The TAC dead time was set to this value to insure that it exceeded that of all other instruments and would be the sole contributor to the dead time. The dead time $\Delta t(n)$ associated with any channel (n) of the MCPHA was readily calculated as a function of the total counts in all channels $(N_{\rm tot})$ and the counts in all channels preceding it in time $[N(n)]$:

$$\Delta t(n)=5\tau N_{\rm tot}+N(n)\tau\ . \tag{2}$$

With the small count rates used for the experiments described in this paper, less than 2000 counts/s, the effective dead time was less than 3% for all channels.

An energy-dependent background was produced during the collection of gas and reference TOF spectra by the impact of high-energy electrons on the exit aperture and skimmer edges and the grid. Low-energy electrons originating from these sources were not attenuated by the gas in the sample cell and arrived in TOF channels corresponding to much higher-energy electrons from the pulsed electron source. This aperture scattering contribution was measured by establishing a retarding field between the pulsed electron source and the sample cell to prevent low-energy electrons originating from the pulsed source from entering the sample cell and reaching the detector. The low-energy TOF spectra recorded this way resulted from high-energy electrons striking aperture edges and causing the ejection of low-energy electrons which were then detected. A correction was applied to the TOF data collected using cell I by subtracting the background produced by exit-aperture scattering from gas and reference TOF spectra. The applied correction resulted in less than a 3% change in the TCS.

Nine individual experiments under varying conditions were averaged to obtain the reported cross section. Sample gas pressure ranged from 0.6 to 2.9 mtorr. Each experiment was weighted according to its statistical significance based on the accumulated counts.

III. ERROR ANALYSIS

A complete description of all contributing errors, except those due to forward scattering and aperture scattering, can be found in an earlier publication.[13] The error sources and their contributions to the uncertainty in the measured total cross section are listed in Table II. All uncertainties reported here are estimated or measured upper bounds to the error or in the cases where standard deviations (σ) were determined from a series of measurements, 2σ errors are quoted.

Careful measures were taken to insure the accuracy of the capacitance manometer used to measure the sample pressure. A Pyrex glass and stainless-steel vacuum system was constructed to calibrate the capacitance manometer for conditions and in the pressure region in which it was used. The estimated accuracy of the gauge was found to be $\pm 1.20\%$ (2σ). The accuracy of the gauge calibration procedure was verified by comparing the results of the calibration of a second capacitance manometer with the results of an independent calibration of the same gauge. The independent calibration performed by Gascoigne and Roberts[14] consisted of comparison of the capacitance manometer with a pressure gauge that had been calibrated using a dead-weight tester. The results of Gascoigne and Roberts indicated that our second capacitance manometer with the head at room temperature was accurate to better than 0.05%. This result is in excellent agreement with our calibration of this capacitance manometer under the same conditions, which indicated that the measured pressure was 1.0024 ± 0.0046 (1σ) times the actual pressure.

The cell length uncertainty was conservatively estimated to be one aperture diameter at each end of the cell. The uncertainty in measured pressure due to pressure gradients in the cell was estimated to be one-half of the maximum observed pressure difference between any two points within the cell. Since cross-section data collected

TABLE II. Summary of contributing errors.

Multiplicative errors (independent of electron energy)				
Pressure measurement (2σ)	$\pm 1.20\%$			
Temperature	$\pm 0.30\%$			
Cell length	$\pm 1.43\%$			
Pressure gradients	$\pm 1.10\%$			
Energy-dependent errors	**1–4 eV**	**4.2–15 eV**	**16–25 eV**	**26–50 eV**
Energy scale errors:				
(i) TOF of energy benchmark (± 500 ps)	$\pm 0.07\%$	$\pm 0.39\%$	$\pm 0.52\%$	$\pm 0.61\%$
(ii) Total electron pathlength (± 0.7 mm)	$\pm 0.11\%$	$\pm 0.17\%$	$\pm 0.17\%$	$\pm 0.15\%$
(iii) Calibration of time base ($\pm 0.05\%$ in time/channel)	$\pm 0.06\%$	$\pm 0.06\%$	$\pm 0.06\%$	$\pm 0.04\%$
(iv) Contact potentials	$\pm 0.44\%$	$\pm 0.24\%$	$\pm 0.02\%$	$\pm 0.01\%$
Gas purity	$\pm 0.10\%$	$\pm 0.10\%$	$\pm 0.10\%$	$\pm 0.10\%$
Entrance-aperture scattering	$+, -0.01\%$	-0.01%	-0.01%	-0.01%
Exit-aperture scattering		$+0.33\%$	$+0.77\%$	$+2.19\%$
Forward scattering	$+0.01\%$	$+0.77\%$	$+0.77\%$	$+0.77\%$
Experimental reproducibility (2σ)	$\pm 1.15\%$	$\pm 0.64\%$	$\pm 1.02\%$	$\pm 1.54\%$
Coherent sum	$+6.0\%$	$+6.7\%$	$+7.5\%$	$+9.4\%$
(maximum error)	-6.0%	-5.6%	-5.9%	-6.5%
Incoherent sum	$+2.5\%$	$+2.6\%$	$+2.9\%$	$+4.0\%$
(most probable error)	-2.5%	-2.3%	-2.5%	-2.8%

using each of the three cells was equally weighted to obtain the final results, average cell length and pressure uncertainties for the three cells were used as effective uncertainties.

Errors in the energy scale were most conveniently evaluated with respect to their effect on the magnitude of the measured cross section and are presented in this way in Table II.

Potential variations between metal surfaces along the electrons' path were reduced by using aluminum, exclusively, in the sample-cell construction and coating all parts exposed to low-energy electrons with colloidal graphite. Potential variations within the sample cells were estimated to be less than 5 mV based on the energy resolution achieved with a similar apparatus.[15]

The sample gas was used directly from the tank and special care was taken to maintain its purity which was claimed to be 99.99% by Matheson, the supplier.

The errors resulting from the scattering of high-energy electrons from the edge of the entrance aperture was measured directly by applying a retarding field between the pulsed source and the entrance to the sample cell, as described in Sec. II. Scattering from the entrance aperture produced an error in the measured cross section of less than 0.01%. Production of secondary electrons by high-energy electrons scattering from the edges of the exit aperture, skimmer, and grid resulted in the largest source of uncertainty at higher energies. A correction, estimated to be accurate to ±20%, was applied to the data collected using cell I as described in Sec. II. The intensity of secondary electrons from this source was measured in the same manner for cell III but a correction was not directly applied to the data. This measurement was used to determine the magnitude of the error from this source and was found to be less than 2.19% above 25 eV, less than 0.77% below 25 eV, less than 0.33% below 15 eV, and insignificant below 4 eV. This error always acted to reduce the value of the measured cross section. No systematic difference larger than the statistical uncertainty and the estimated 20% uncertainty in the applied correction to data obtained with cell I was found between the measured cross sections using the three cell configurations. As an upper limit to the uncertainty from this source, the error measured for cell III was used for the average of all the data.

An error, inherent to all transmission experiments, resulted from the failure to sufficiently discriminate against electrons scattered by the sample gas in the forward direction. This error became largest at higher energies where inelastic and elastic scattering were dominated by small-angle scattering. By varying the acceptance angle of the detector and modeling the forward scattering, the error from this source was estimated.

The measured total cross section (Q) was the total, elastic and inelastic, differential cross section integrated over all angles against which the experiment discriminated, and averaged over the cell length:

$$Q_{\text{meas}}=\frac{1}{L}\int_0^L dx\int_0^{2\pi} d\phi\int_{\omega(x)}^{\pi} d\theta\sin\theta\left[\left[\frac{d\sigma}{d\Omega}\right]_{\text{el}}+\left[\frac{d\sigma}{d\Omega}\right]_{\text{inel}}\right], \tag{3}$$

where $\omega(x)$ is the acceptance angle of the detector as a function of location along the center line in the sample cell, and L is the sample-cell length. The factional error in the measured cross section was

$$\Delta Q/Q=\frac{2\pi}{L}\int_0^L dx\int_0^{\omega(x)} d\theta\sin\theta\left[\left[\frac{d\sigma/d\Omega}{Q}\right]_{\text{el}}+\left[\frac{d\sigma/d\Omega}{Q}\right]_{\text{inel}}\right]. \tag{4}$$

The elastic differential cross section for H_2 at 60 eV reported by Trajmar *et al.*[16(a)] was derived from relative measurements made by Srivastava *et al.*[16(b)] Since their data do not extend below 20°, they were extrapolated to zero angle assuming exponential behavior in order to estimate the error due to small-angle elastic scattering. This extrapolation scheme predicted a larger small-angle scattering contribution than the extrapolation method employed by Trajmar *et al.* Consequently, the calculated error from this source is probably an overestimate.

The inelastic contribution was derived in an identical manner from the experimental data of Srivastava *et al.*[17] for the excitation of the $B\,^1\Sigma_u^+(v'=2)$ state for 60-eV incident electrons. This single transition was used to approximate the angular behavior of all inelastic processes.

The relative contributions of elastic and inelastic cross sections to the total was based on the calculation of van Wingerden *et al.*,[8] who found 43% elastic contribution and 57% inelastic contribution at 60 eV. At lower energies the error was expected to be less than at 60 eV so the calculated error was used as an upper bound for energies above the electronic threshold. Below threshold the fraction of forward scattering was calculated assuming that all scattering was isotropic.

The reproducibility of the experiment reflected all systematic errors that were affected by the variation of experimental parameters, statistical counting errors, and errors that were random between experiments. The uncer-

tainty at each point based on the reproducibility (σ equals rms deviation) was comparable to the uncertainty in the weighted average of the nine experiments based on counting statistics [$\sigma=(\text{count})^{1/2}$].

A summary of all error sources and their effect on the total cross section is presented in Table II. The coherent sum represents a direct sum of all listed errors and acts as an upper limit estimate to the actual error. The incoherent sum was obtained by adding directly those errors that could only act in one direction, adding the square of this sum to the sum of the squares of the remaining errors, and taking the square root of this total sum. The incoherent sum represents the most probable estimate of the accuracy of the experiment.

IV. RESULTS

The total cross-section measurements are tabulated and compared with other experimental and theoretical values in Table III. The reported results were obtained at the listed energies by performing a linear interpolation between the two closest experimentally determined points. No attempt was made to resolve the resonance structure above 10 eV.[18] Experiments and theory have indicated that a very broad short-lived shape resonance, corresponding to the $^2\Sigma_u^+$ state of H_2^-, occurs around 3 eV, in the region of the broad maximum in the total cross section.[19]

The measurements of Golden *et al.*,[10] obtained with a Ramsauer-type apparatus, are in agreement with the present results for energies below 4 eV; however, a deviation grows with increasing energy. Between 8 and 15 eV the measurements of Golden *et al.* are smaller than the present measurement by a nearly constant 12%. This difference is much larger than the combined error of the present experiment and the ±3% error quoted by Golden *et al.* Bederson and Kieffer[20] in a critical review suggested that an error greater than 5—10% is a more realistic estimate for the measurement of the helium cross section by Golden and Bandel.[21] Since the same apparatus and error analysis were employed for both the helium and hydrogen measurements, the comment of Bedeson and Kieffer is equally applicable to Golden *et al.*'s measurement of the hydrogen cross section. A total systematic error of the magnitude suggested would account for the observed difference between the present results and the results of Golden *et al.* The ±3% error quoted by Golden *et al.* resulted from taking the square root of the sum of the squares of contributing systematic errors and can be viewed in the context of this paper as the most probable error. If a direct sum of contributing errors is employed to obtain a maximum error, then the combined maximum errors of Golden *et al.* (±7%) and the present results (−5.6%) account for the deviation between these two

TABLE III. Total cross-section values for H_2 in Å^2. Quoted errors are as follows. Dalba *et al.*: 3.5% ($E \leq 1$ eV), 2.0% ($1.2 \leq E \leq 50$ eV). Deuring *et al.*: 5% (systematic only). Hoffman *et al.*: $\leq 1.2\%$ ($E < 50$ eV); 2.5% ($E = 50$ eV). van Wingerden *et al.*: 3.1%.

Energy	Present results	Dalba *et al.*[a]	Deuring *et al.*[b]	Hoffman *et al.*[c]	van Wingerden *et al.*[d]	Hara[e]	Feldt and Morrison[f]
1.0	13.26	14.00				12.709	13.44
1.2	13.85						
1.4	14.40						
1.5	14.62	15.37					14.91
1.6	14.86					14.157	
1.8	15.26						
2.0	15.58	16.16		17.0			15.95
2.2	15.99						
2.4	16.14						
2.5	16.27	16.66				15.752	
2.6	16.30						
2.8	16.40						
2.9	16.46			17.3			
3.0	16.46						16.37
3.2	16.48						
3.4	16.41						
3.5	16.36						
3.6	16.32						
3.8	16.20						
3.9	16.19			17.6			
4.0	16.10	15.79				15.338	
4.5	15.67						15.57
4.9	15.30			15.6			
5.0	15.20						
5.5	14.70						
6.0	14.16	14.23	13.01				13.97
6.5	13.66						
6.8	13.35			14.3		13.259	

TABLE III. (*Continued*).

Energy	Present results	Dalba *et al.*[a]	Deuring *et al.*[b]	Hoffman *et al.*[c]	van Wingerden *et al.*[d]	Hara[e]	Feldt and Morrison[f]
7.0	13.14		12.48				
7.5	12.68						
8.0	12.18	12.35	12.02				11.92
8.5	11.76						
8.8	11.50			12.2			
9.0	11.33		10.80				
9.5	10.98						
9.8	10.75					10.546	
10.0	10.60	10.78	10.49				10.21
10.8	10.03			10.56			
11.0	9.884		9.80				
12.0	9.317		8.79				
12.9	8.857			9.48			
13.0	8.809		8.18				
14.0	8.503		8.13				
14.9	7.951			8.48			
15.0	7.911	8.205	8.12				
16.0	7.518						
18.0	6.899						
20.0	6.378	6.553		6.72			
25.0	5.408		5.22	5.79	5.75		
30.0	4.776	5.013	4.75	4.92	4.89		
35.0	4.300			4.66	4.44		
40.0	3.936	4.229	4.06	4.30	4.00		
45.0	3.641			3.98	3.86		
50.0	3.402	3.809	3.42	3.66	3.62		

[a]Reference 9.
[b]Reference 11.
[c]Reference 6.
[d]Reference 8.
[e]Reference 22.
[f]Reference 23.

measurements above 8 eV. It is the opinion of the author that this does not constitute agreement between the two measurements; the measurements would only be in agreement in the improbable case that all identified systematic errors acted in phase in both experiments. A more probable situation is that unidentified or underestimated systematic errors were present in the earlier measurement.

The measurements of Ferch *et al.*,[7] obtained with a TOF transmission spectrometer, are, on average, 4% less than the present results, but well within the combined errors.

Linear transmission experiments employing electrostatic energy analyzers were used by Dalba *et al.*,[9] and van Wingerden *et al.*[8] Though agreement is good below 40 eV, the measurements of Dalba *et al.* exceed the present results at higher energies by as much as 12%. The measurements of van Wingerden *et al.*, above 25 eV, are in good agreement with the present results. The apparatus used by Hoffman *et al.*[6] incorporated a curved solenoid in the sample cell. Their measurements are consistently larger than the present measurements at all energies by an average of 6.3%.

Agreement is good between the present results of those of Duering *et al.*[11] using a linear transmission cell and a cylindrical mirror spectrometer with a relatively low-energy resolution ($\Delta E \geq 1$ eV). They report both a total systematic error of 5%, which is a direct sum of contributing systematic errors, and a random error (1σ) varying from 2.1% to 0.3%. Individual points differ from the present results by as much as 8% but systematic differences (i.e., when the deviation is averaged over a number of data points) are around 4% for energies less than 15 eV and much less at higher energies.

Two theoretical cross sections are also presented for comparison. Hara[22] calculated the integral elastic cross section using a fixed-nuclei adiabatic-exchange approximation (polarization and exchange included). In order to compare Hara's results with the present experimental values, consideration must be given to the vibrationally inelastic contribution to the total cross section. The single most dominant contribution to the inelastic cross section below the electronic threshold is the cross section for excitation to the first vibrational level, which reaches a maximum of about 0.4 Å^2 around 3 eV.[17] Taking this inelastic contribution into account, the elastic cross section calculated by Hara is in agreement with the present results.

Feldt and Morrison[23] calculated the total cross section including vibrational and rotational excitations from the

$j=0$, $v=0$ up to the $j=2$, $v=2$ state. Adiabatic nuclei calculations including exact static exchange with polarization were used for the elastic contribution and a full rovibrational laboratory-frame close-coupling calculation with exchange and polarization was employed to obtain the inelastic contribution. Their results are in good agreement at all energies except at 10 eV where they are 3.7% below the present measurements.

ACKNOWLEDGMENTS

The author would like to thank Dr. R. A. Bonham and Dr. W. G. Wilson for invaluable assistance in all aspects of this work. This work has been supported by the National Science Foundation Grant No. CHE-80-00253 made to the Indiana University Foundation, Bloomington, Indiana 47402.

[1]K. D. Jordan, J. A. Michejde, and P. D. Burrow, Chem. Phys. Lett. **42**, 227 (1976).

[2]G. J. Schulz, in *Principles of Laser Plasmas,* edited by G. Bekefi (Wiley, New York, 1976), Chap. 2.

[3]L. G. Christophorou, in *Proceedings of the XIIIth International Conference on Phenomena in Ionized Gases, Berlin, 1977* (Physical Society of GDR, Berlin, 1977), Pt. 2, p. 51.

[4]J. L. Dehmer and D. Dill, in Argonne National Laboratory Report No. ANL-77-65 (unpublished).

[5]N. F. Lane, Rev. Mod. Phys. **52**, 29 (1980).

[6]K. R. Hoffman, M. S. Dababnech, Y. F. Hsieh, W. E. Kauppila, V. Pol, J. H. Smart, and T. S. Stein, Phys. Rev. A **25**, 1393 (1982).

[7]J. Ferch, W. Raith, and K. Schöder, J. Phys. B **13**, 1481 (1982).

[8]B. van Wingerden, R. W. Wagenaar, and F. J. de Heer, J. Phys. B **13**, 3481 (1980).

[9]G. Dalba, P. Fornasini, I. Lazzizzera, G. Ranieri, and A. Zecca, J. Phys. B **13**, 2839 (1980).

[10]D. E. Golden, H. W. Bandel, and J. A. Salerno, Phys. Rev. **146**, 40 (1966).

[11]A. Deuring, K. Floeder, D. Fromme, W. Raith, A. Schwab, G. Sinapius, P. W. Zitzewitz, and J. Krug, J. Phys. B **16**, 1633 (1983).

[12]R. E. Kennerly and R. A. Bonham, Phys. Rev. A **17**, 1844 (1978).

[13]Robert K. Jones and R. A. Bonham, Aust. J. Phys. **35**, 559 (1982).

[14]The author would like to thank John Gascoigne and Kevin Roberts of the Australian National University, Institute of Advanced Studies, for the calibration of our MKS capacitance manometer.

[15]S. R. Long, J. T. Meek, and J. P. Reilly, J. Chem. Phys. **79**, 3206 (1983).

[16](a) S. Trajmar, D. F. Register, and A. Chutjian, Phys. Rep. **97**, 219 (1983); (b) S. K. Srivastava, A. Chutjian, and S. Trajmar, J. Chem. Phys. **63**, 2659 (1975).

[17]S. K. Srivastava and S. Jensen, J. Phys. **45**, 423 (1973).

[18]G. J. Schulz, Rev. Mod. Phys. **45**, 423 (1973).

[19]See, for example, G. J. Schulz and R. K. Asundi, Phys. Rev. **158**, 25 (1967).

[20]B. Bederson and L. J. Kieffer, Rev. Mod. Phys. **43**, 601 (1971).

[21]D. E. Golden and H. W. Bandel, Phys. Rev. **138**, A14 (1965).

[22]S. Hara, J. Phys. Soc. Jpn. **27**, 1009 (1969).

[23]A. N. Feldt and M. A. Morrison (unpublished). The theory and potentials are described in M. A. Morrison, A. N. Feldt, and D. Austin, Phys. Rev. A **29**, 2518 (1984).